*Nat Chem Biol*. Author manuscript; available in PMC 2014 April 01.

Published in final edited form as:
*Nat Chem Biol*. 2013 October ; 9(10): 607–609. doi:10.1038/nchembio.1311.

# Spontaneous activation of [FeFe]-hydrogenases by an inorganic [2Fe] active site mimic

**Julian Esselborn**[1], **Camilla Lambertz**[#1], **Agnieszka Adamska-Venkates**[#2], **Trevor Simmons**[#3], **Gustav Berggren**[3,4], **Jens Noth**[1], **Judith Siebel**[2], **Anja Hemschemeier**[1], **Vincent Artero**[3], **Edward Reijerse**[2], **Marc Fontecave**[3,5], **Wolfgang Lubitz**[2], and **Thomas Happe**[1,*]

[1]Ruhr-Universität Bochum, Fakultät für Biologie und Biotechnologie, Lehrstuhl für Biochemie der Pflanzen, AG Photobiotechnologie, 44801 Bochum, Germany.

[2]Max-Planck-Institut für Chemische Energiekonversion, Stiftstrasse 34-36, 45470 Mülheim an der Ruhr, Germany.

[3]Laboratoire de Chimie et Biologie des Métaux (CEA / Université Grenoble 1 / CNRS), 17 rue des Martyrs, F-38054 Grenoble cedex 9, France.

[5]Collège de France, 11 Place Marcelin Berthelot, 75231 Paris Cedex 05, France

[#] These authors contributed equally to this work.

## Abstract

Hydrogenases catalyze the formation of hydrogen. The cofactor (H-cluster) of [FeFe]-hydrogenases consists of a [4Fe-4S]-cluster bridged to a unique [2Fe]-subcluster whose biosynthesis *in vivo* requires hydrogenase-specific maturases. Here we show that a chemical mimic of the [2Fe]-subcluster can reconstitute apo-hydrogenase to full activity, independent of helper proteins. The assembled H-cluster is virtually indistinguishable from the native cofactor. This procedure will be a powerful tool for developing novel artificial $H_2$-producing catalysts.

Research on hydrogenase enzymes has gained considerable interest as these biocatalysts efficiently produce molecular hydrogen ($H_2$). In order to develop inexpensive but highly active chemical mimics, detailed knowledge about the structure, reaction mechanism and assembly of the active site in these enzymes is required. Hydrogenases of the [FeFe]-type (HYDA) are the most active $H_2$ producers[1]. They contain a complex cofactor, the "H-cluster", consisting of a simple cubane [4Fe-4S]-cluster bound via cysteine to a unique [2Fe]-subcluster in which two [Fe]-atoms are coordinated by CO, CN- and a dithiolate.[2,3] (Fig. 1). In the living cell, biosynthesis of the [2Fe]-subcluster requires only three hydrogenase-specific maturases, HYDE, HYDF and HYDG[4]. HYDF is the scaffold for [2Fe]-subcluster assembly and transfers the cluster to the HYDA protein containing a pre-assembled [4Fe-4S]-cluster (apoHYDA)[2,5,6]. Numerous model compounds have been synthesized to investigate different features of the [2Fe]-subcluster[7]. All of the mimics tested so far, including the most structurally relevant ones[8,9], have only low $H_2$ evolving

[*]Correspondence to: Thomas Happe, Address: Ruhr-Universität Bochum, Lehrstuhl für Biochemie der Pflanzen, AG Photobiotechnologie, ND2/169, 44801 Bochum, Germany. Phone: +49 234 32 27026. Fax: +49 234 32 14322. thomas.happe@rub.de. .

[4]Current address: Dept. of Biochemistry and Biophysics, Stockholm University, Svante Arrhenius väg 16, 106 91 Stockholm, Sweden

**Author Contributions** C.L., J.E., J.N., A.H., M.F., W.L. and T.H. conceived and designed experiments. C.L., J.S., J.E., J.N. and A.A. performed the experiments. C.L., J.E., A.H., A.A. and T.H. analyzed the data. G.B., T.S., V.A. and M.F. provided the $[2Fe]^{MIM}$ and $[2Fe]^{pdt}$ complexes. A.A., E.R. and W.L. performed and analyzed the EPR and FTIR experiments. All authors discussed the results. A.H., J.E. and T.H. wrote the manuscript.

**Competing Financial Interests** The authors declare no competing financial interests.


Europe PMC Funders Author Manuscripts

efficiencies *in vitro*. A major challenge is therefore to understand the role of the protein environment in allowing the inorganic clusters to come to full activity[10]. Notably, a synthetic mimic of the [2Fe]-subcluster can be loaded onto HYDF from *Thermotoga maritima in vitro*[11]. This artificially loaded HYDF is able to transfer the di-iron analogues to the apo-form of [FeFe]-hydrogenase HYDA1 from *Chlamydomonas reinhardtii* (apoHYDA1), resulting in a fully active hydrogenase[11].

Little is known about the mechanistic details of the transfer of the [2Fe]-subcluster from HYDF to apoHYDA. However, a function of HYDF in inserting the [2Fe]-subcluster in addition to serving as the scaffold for cluster assembly has been presumed to date. We tested if a [2Fe]-subsite mimic containing an azadithiolate bridge ($[2Fe]^{MIM}$; Fig. 1)[9,11] would be able to integrate into the HYDA1 apo-protein in the absence of HYDF. We combined inactive apoHYDA1 heterologously produced in *Escherichia coli* with pure $[2Fe]^{MIM}$ solutions. Remarkably, this procedure resulted in high specific hydrogenase activities (Fig. 2a) despite the absence of helper-proteins like HYDF. Both the resulting activities and the molar excess of $[2Fe]^{MIM}$ required to achieve these were similar to or even better than those obtained using $[2Fe]^{MIM}$-loaded HYDF ($HYDF^{MIM}$)[11] (Fig. 2a). A 2.5-fold excess of $[2Fe]^{MIM}$ over apoHYDA1 sufficed to yield a specific activity as high as HYDA1 maturated in *Clostridium acetobutylicum*, an established host for heterologous production of active [FeFe]-hydrogenases[10] (Fig. 2b). This indicates that the $[2Fe]^{MIM}$ compound was able to autonomously integrate into apoHYDA1 very efficiently.

In contrast to *C. reinhardtii* HYDA1, which consists only of the H-cluster containing H-domain, most bacterial HYDA proteins possess further domains holding additional [FeS]-clusters[3,12]. The spontaneous integration of $[2Fe]^{MIM}$ into algal apoHYDA1 might therefore be restricted to these single-domain proteins and not suited for broad applications. The crystal structure of *C. reinhardtii* apoHYDA1 revealed a positively charged channel connecting the protein surface to the active site niche[5]. As this channel is not observed in holoHYDA enzymes[3,13] it might serve as the entry pathway for the [2Fe]-subcluster, closing upon its attachment to the [4Fe-4S]-site. In multi-domain HYDA enzymes the entry-site of the [2Fe]-compound might be obstructed, making a chaperone or maturase indispensable for integrating the [2Fe]-subcluster. Therefore we examined the activity of enzymes from *Megasphaera elsdenii* ($HYDA_{Me}$) and *C. pasteurianum* (CpI) after treatment with $[2Fe]^{MIM}$. These have two and four additional [FeS]-clusters, respectively, and accordingly longer N-termini[3,14]. In both cases the apo-enzymes produced in *E. coli* did not show any $H_2$ evolution activity. However, after *in vitro* maturation with $[2Fe]^{MIM}$, specific activities of 308±40 and 2,037±616 μmol $H_2 \cdot$ mg $HYDA^{MIM\text{-}1} \cdot min^{-1}$ were achieved by $HYDA_{Me}{}^{MIM}$ and $CpI^{MIM}$, respectively (Fig. 2b). These activities were in a similar range as those of native *M. elsdenii* HYDA[15] and heterologously produced CpI[10].

We also tested if $HYDA1^{MIM}$ would be able to interact with its natural electron delivery systems. The cellular electron donor of HYDA1 is ferredoxin PETF, and in illuminated algae, the major electron source for $H_2$ production is photosystem 1 (PS1)[16]. In the dark, pyruvate oxidation and subsequent PETF reduction by pyruvate:ferredoxin oxidoreductase (PFR1) are responsible for $H_2$ generation in *Chlamydomonas*[17]. Using *in vitro* assays in which either PS1 or PFR1 were used as PETF reducing components, $H_2$ evolution activities of $HYDA1^{MIM}$ and HYDA1 were the same (Fig. 2c). The comparable rate of electron transfer between PETF and HYDA1 or $HYDA1^{MIM}$ suggests very similar structural properties and indicates that the *in vivo* functionality of $HYDA1^{MIM}$ is identical to native HYDA1.

Electron paramagnetic resonance (EPR) and Fourier transform infrared (FTIR) spectroscopy give detailed information about the electronic structure of the H-cluster and the state of the

CO and $CN^-$ ligands, respectively[18]. Therefore, we examined the reconstituted and subsequently purified $HYDA1^{MIM}$ protein by both methods (Fig. 3). In order to obtain well-defined EPR and FTIR spectra of the H-cluster, we treated $HYDA1^{MIM}$ with CO to generate the characteristic $H_{ox}$-CO state. Indeed, the EPR spectrum of this preparation (Fig. 3a) unequivocally identified it as the native $H_{ox}$-CO state[19]. Also its FTIR spectrum (Fig. 3b) showed the CO and $CN^-$ bands at the positions previously observed for the native $H_{ox}$-CO state[20]. For comparison, Fig. 3 also shows the EPR and FTIR spectra of the starting materials, i.e. apoHYDA1 (Fig. 3a) and $[2Fe]^{MIM}$ (Fig. 3b). EPR spectra of apoHYDA1 indicated typical *g*-values for [4Fe-4S]-clusters and were very similar to the values observed for apoHYDA1 previously[6] (Fig. 3a). The shift of the FTIR bands when going from free $[2Fe]^{MIM}$ to $HYDA1^{MIM}$-CO (Fig 3b) is consistent with the change of the ligand geometry occurring upon integration of $[2Fe]^{MIM}$ into the polypeptide, which involves its attachment to the [4Fe-4S]-cluster and rearrangement of one CO ligand into a bridging Fe-CO-Fe position (see Fig. 1). In the as-isolated form, [FeFe]-hydrogenases usually show a mixture of redox states, which represent the different electronic configurations of individual steps of the catalytic cycle[19]. In EPR (Fig. 3a) and FTIR (Fig. 3b) spectra of untreated $HYDA1^{MIM}$, these signals were also observed. Again, peak shapes and *g*-tensor values corresponded well to previously published data[19,20,21]. The spectroscopic data therefore show that the spontaneous integration of $[2Fe]^{MIM}$ into the apoHYDA1 protein results in an H-cluster virtually identical to the native one.

One of the four CO ligands of $[2Fe]^{MIM}$ must dissociate to yield active $HYDA1^{MIM}$ (Fig. 1). We verified the release of CO spectroscopically by monitoring the binding of free CO to deoxyhemoglobin over time. This hemoglobin-based assay can sensitively detect dissolved CO[22]. Indeed, the typical CO-induced shift of the hemoglobin Soret band occurred when apoHYDA1 and $[2Fe]^{MIM}$ were mixed (Supplementary Results, Supplementary Fig. 1a) and the reaction was complete after 2-3 minutes. The release of CO depended linearly on the apoHYDA1 concentration (Supplementary Fig. 1b). We estimated that approximately 0.6 moles of CO were released per mol apoHYDA1.

To test if the spontaneous integration of the [2Fe]-subcluster reported here was strictly specific for the native cofactor $[2Fe]^{MIM}$, carrying a secondary amine as the dithiolate bridgehead, we attempted to integrate a similar mimic into apoHYDA1. $[2Fe]^{pdt}$ features a 1,3-propanedithiolate and thus differs from $[2Fe]^{MIM}$ only by the head atom of the bridging dithiolate, which is a carbon instead of a nitrogen in this case. $[2Fe]^{pdt}$, transferred to apoHYDA1 by HYDF, does not form an active H-cluster[11]. After treating apoHYDA1 with $[2Fe]^{pdt}$ in the absence of HYDF, we could measure no hydrogenase activity accordingly. However, the FTIR spectrum of $HYDA1^{pdt}$ proved the presence of $[2Fe]^{pdt}$ within the protein (Supplementary Fig. 3). In contrast to $HYDA1^{MIM}$ which shows a mixture of states (Fig. 3b) $HYDA1^{pdt}$ is stabilized as a single species resembling the native $H_{ox}$-state (compare Supplementary Fig. 2b and Supplementary Fig. 3)[11]. The unassisted integration of $[2Fe]^{pdt}$ shows that the [2Fe]-subcluster integration is not strictly selective. This property could open new avenues to investigate other synthetic cluster derivatives in a protein environment.

In conclusion, the results presented here show that, under *in vitro* conditions, no [2Fe]-subcluster transferase is needed for HYDA activation and, therefore, offer novel insights into the *in vivo* maturation process of [FeFe]-hydrogenases. They indicate that after synthesis of the [2Fe]-subsite precursor and its transfer to apoHYDA the last three steps of HYDA activation might also naturally occur without further assistance of maturases. First, the [2Fe]-subcluster must find its way from the protein surface to the pre-assembled [4Fe-4S]-cluster. It was suggested that the water-filled channel reaching from the protein surface to the [4Fe-4S]-cluster in apoHYDA1[5] might allow an entropically driven insertion

of the [2Fe]-subcluster[23]. Charged residues lining the channel surface are suitable candidates for interacting with the [2Fe]-subsite and directing its steric orientation by providing the correct electrostatic attracting and repelling forces[23]. Once the [2Fe]-subcluster is positioned at the end of the channel, coordination via a bridging residue to the [4F-e4S]-cluster is required. The coordination of a thioether ligand onto [2Fe] mimics can be oxidatively induced, yielding an intermediate species with a structure closely related to the $H_{ox}$-CO state[24]. Finally, the fourth CO-ligand present in $[2Fe]^{MIM}$, and probably also in the naturally synthesized [2Fe]-subcluster present on HYDF[6], dissociates. At which step of H-cluster assembly this happens remains to be elucidated. A transient formation of the $H_{ox}$-CO state, followed by the release of the excess CO-ligand might be suggested.

Biochemists have long been fascinated by the structure of the [2Fe]-subcluster which, apart from the cysteinyl bridge, has only non-covalent interactions with the protein. One cannot resist the idea that the [2Fe]-subsite may originate from an inorganic complex that spontaneously formed in the pre-biotic world as suggested earlier[12]. Both HYDF-assisted[11] and the here reported unassisted integration of $[2Fe]^{MIM}$ and $[2Fe]^{pdt}$ into apoHYDA1 are powerful demonstrations of the synergy between chemistry and biology. Given the enormous efforts made over the years in both biomimetic chemistry of the [2Fe]-subcluster[7] and the elucidation of the functional aspects of the HYDA protein matrix[25], bridging the gap between the two fields promises new insights into the chemistry of [FeFe]-hydrogenases. Moreover, the HYDF-independent procedure described here opens up novel areas for hydrogenase research. To date, only a subset of HYDA enzymes has been analyzed in biochemical and biophysical detail, due to the difficulty of generating large amounts of fully active enzymes. The ability to reconstitute apo-hydrogenases even in the absence of maturation factors now permits the analysis of the whole spectrum of HYDA sequences.

In particular the chaperone-independent assembly of (synthetic) clusters will allow us to unravel protein-based structure-function relationships from an entirely new perspective. To date, these are investigated by site-directed mutagenesis of the protein. But with a system of spontaneous cluster assembly at hand, attempts can be made to engineer and test artificial protein environments. This might result in entirely artificial hydrogenases with applications in bio-hydrogen production and bio-fuel cell technology.

## Online methods

### Heterologous expression and purification of proteins

ApoHYDA1 and apoCpI were produced anaerobically in *Escherichia coli* BL21(DE3) Δ*iscR*[26] making use of optimized sequences and the pET expression system as described earlier[27], but without co-expression of maturase genes. *M. elsdenii HYDA* was expressed accordingly after cloning of $HYDA_{Me}$ from pT7HME[14] into pTSH_hydA1Cr_STII[28]. Purification of hydrogenases was carried out under strictly anaerobic conditions using a one-step strep-tactin affinity chromatography protocol as described earlier with minor modifications[28]. Heterologous synthesis of active HYDA1 in *Clostridium acetobutylicum* ATCC82414[28], isolation of PSI[29] and plastocyanin from *C. reinhardtii*[30] as well as heterologous expression of PETF[16] and PFR1[17] in *E. coli* were described earlier.

### Preparation of $[2Fe]^{MIM}$ and $[2Fe]^{pdt}$

Synthesis of $[2Fe]^{MIM}$ and $[2Fe]^{pdt}$ [31,32] followed the previously published protocol[9], in the case of $[2Fe]^{pdt}$ with modifications as described earlier[11]. Crystalline compounds were dissolved in 20 mM HEPES pH 7.5, 100 mM KCl, handled strictly anaerobically and stored at −80°C.

### *In vitro* maturation of [FeFe]-hydrogenases

*In vitro* maturation of hydrogenases was achieved by incubating 800 ng apo-protein (0.04 μM HYDA1) under strictly anaerobic conditions in 400 μl of 0.1 M potassium phosphate buffer, pH 6.8, with 2 mM sodium dithionite (NaDT) at 25°C for 30 min with a 10-fold molar excess of $[2Fe]^{MIM}$ if not stated otherwise. Subsequent *in vitro* activity measurements using NaDT-reduced methyl viologen as artificial electron donor were done as previously described[33]. Maturation of $HYDA1^{MIM}$ for EPR and FTIR measurements was carried out with 150 μM apoHYDA1. The protein was subsequently purified and re-buffered to 0.01 M Tris-HCl, pH 8.0, 2 mM NaDT, by size exclusion chromatography using a NAP™ 5 column (GE Healthcare) and concentrated to 500 μM for EPR and FTIR measurements using Amicon Ultra centrifugal filters 10K (Millipore). Spectra of 12 mM $[2Fe]^{MIM}$ were recorded in 20 mM HEPES buffer pH 7.5, 100 mM KCl.

### Pyruvate driven and light driven hydrogen evolution assays

Each pyruvate-driven reaction contained PFR1, PETF and *C. reinhardtii* HYDA1 or $HYDA1^{MIM}$, pyruvate and acetylCoA in potassium phosphate buffer, pH 6.8, as described earlier[17]. The reaction mixtures were incubated for 30 min at 37°C before analyzing the amount of $H_2$ in the gas phase. For light-driven measurements, PSI and plastocyanin from *C. reinhardtii*, ascorbate and dichlorophenolindophenol were combined with HYDA1 or $HYDA1^{MIM}$ and PETF as previously published[16]. These reaction mixtures were illuminated for 30 min at 30°C using monochromatic white and red light (250 μEinstein).

### Detection of CO by a hemoglobin-based assay

Bovine hemoglobin (Sigma-Aldrich) was reduced to deoxyhemoglobin (Hb) under strictly anaerobic conditions with NaDT and was brought to ~ 4.5 μM hemoglobin in 100 mM potassium phosphate buffer pH 6.8 with 2 mM NaDT. Spectra and single wavelength kinetics were taken with a UV-2450 spectrophotometer (Shimadzu) at room temperature in sealed 1 ml micro UV-cuvettes to keep anaerobic conditions. $[2Fe]^{MIM}$ was added with gastight syringes (Hamilton) from sealed, anaerobic vials to 10 times the intended concentration of apoHYDA1 (2 μM if not stated otherwise). After each injection thorough mixing was ensured by inverting the cuvette several times. During the whole process the absorbance at 419 nm characteristic for the maximum of the Soret peak of carbonmonoxyhemoglobin (HbCO) was recorded. Concentrations of HbCO were calculated using the difference of the molar absorption coefficients of Hb and HbCO at 419 nm, which can be calculated from spectra of known concentrations of fully reduced Hb and fully saturated HbCO, respectively. The heme concentration could accurately be measured using published molar absorption coefficients of characteristic bands in the visible range[34].

### EPR and FTIR analyses

FTIR spectra were obtained with a Bruker IFS 66v/s FTIR spectrometer equipped with a Bruker MCT (mercury cadmium telluride) detector. The spectra were accumulated in the double-sided, forward-backward mode with 1000 scans and a resolution of 2 $cm^{-1}$ at 15°C. Data processing was facilitated by home written routines in the MATLAB program environment.

Q-band EPR spectra were measured using the 2 pulse echo-detected EPR technique. The length of the π/2 and π MW pulses were set to 16 ns and 32 ns respectively, separated with τ = 500ns. The shot repetition time was set to 1 ms. All measurements were performed on a home build Q-band pulse spectrometer. The temperature was controlled in a custom-built cryofree cryostat from Advanced Research Systems (base temperature 8 K). The sample was accommodated in a homebuilt Q-band ENDOR resonator insert[35].

### Statistical analyses

All hydrogenase activity tests were done at least four times. Values shown are averages, error bars show the standard deviations. EPR and FTIR analyses were done on two independently prepared samples.

## Supplementary Material

Refer to Web version on PubMed Central for supplementary material.

## Acknowledgments

This work was supported by the Bundesministerium für Bildung und Forschung (BMBF) (Bio-H2) (to T.H. and W.L.), the Max Planck Society, the French National Research Agency (ANR, NiFe–Cat ANR–10–BLAN–711 and Labex program ARCANE, 11– LABX–003) (to T.S.,V.A and M.F) and the European Research Council under the European Union's Seventh Framework Programme (FP/2007-2013/ERC Grant Agreement n.306398) (to V.A.). GB gratefully acknowledges Bengt Lundqvist minnesfond, FORMAS (contract number 213-2010-563) and the Swedish royal academy of sciences. T.H. gratefully acknowledges support from the Deutsche Forschungsgemeinschaft (HA 255/2-1) and the Volkswagen foundation (LigH2t). J.E. is financed by the Studienstiftung des deutschen Volkes.

## References

1. Frey M. Hydrogenases: hydrogen-activating enzymes. ChemBioChem. 2002; 3:153–160. [PubMed: 11921392]
2. Peters JW, Broderick JB. Emerging paradigms for complex iron-sulfur cofactor assembly and insertion. Annu. Rev. Biochem. 2012; 81:429–450. [PubMed: 22482905]
3. Peters JW, Lanzilotta WN, Lemon BJ, Seefeldt LC. X-ray crystal structure of the Fe-only hydrogenase (CpI) from *Clostridium pasteurianum* to 1.8 angstrom resolution. Science. 1998; 282:1853–1858. [PubMed: 9836629]
4. Posewitz MC, et al. Discovery of two novel radical S-adenosylmethionine proteins required for the assembly of an active [Fe] hydrogenase. J. Biol. Chem. 2004; 279:25711–25720. [PubMed: 15082711]
5. Mulder DW, et al. Stepwise [FeFe]-hydrogenase H-cluster assembly revealed in the structure of $HydA^{\Delta EFG}$. Nature. 2010; 465:248–251. [PubMed: 20418861]
6. Czech I, Silakov A, Lubitz W, Happe T. The [FeFe]-hydrogenase maturase HydF from *Clostridium acetobutylicum* contains a CO and CN- ligated iron cofactor. FEBS Lett. 2010; 584:638–642. [PubMed: 20018187]
7. Tard C, Pickett CJ. Structural and functional analogues of the active sites of the [Fe]-, [NiFe]-, and [FeFe]-hydrogenases. Chem. Rev. 2009; 109:2245–2274. [PubMed: 19438209]
8. Tard C, et al. Synthesis of the H-cluster framework of iron-only hydrogenase. Nature. 2005; 433:610–613. [PubMed: 15703741]
9. Li H, Rauchfuss TB. Iron carbonyl sulfides, formaldehyde, and amines condense to give the proposed azadithiolate cofactor of the Fe-only hydrogenases. J. Am. Chem. Soc. 2002; 124:726–727. [PubMed: 11817928]
10. Knörzer P, et al. Importance of the protein framework for catalytic activity of [FeFe]-hydrogenases. J. Biol. Chem. 2012; 287:1489–1499. [PubMed: 22110126]
11. Berggren G, et al. Biomimetic assembly and activation of [FeFe]-hydrogenases. Nature. 2013 in press.
12. Meyer J. [FeFe] hydrogenases and their evolution: a genomic perspective. Cell. Mol. Life Sci. 2007; 64:1063–1084. [PubMed: 17353991]
13. Nicolet Y, Piras C, Legrand P, Hatchikian CE, Fontecilla-Camps JC. *Desulfovibrio desulfuricans* iron hydrogenase: the structure shows unusual coordination to an active site Fe binuclear center. Structure. 1999; 7:13–23. [PubMed: 10368269]
14. Atta M, Meyer J. Characterization of the gene encoding the [Fe]-hydrogenase from *Megasphaera elsdenii*. Biochim. Biophys. Acta. 2000; 1476:368–371. [PubMed: 10669801]

15. van Dijk C, Veeger C. The effects of pH and redox potential on the hydrogen production activity of the hydrogenase from *Megasphaera elsdenii*. Eur. J. Biochem. 1981; 114:209–219. [PubMed: 7011807]
16. Winkler M, Kuhlgert S, Hippler M, Happe T. Characterization of the Key Step for Light-driven Hydrogen Evolution in Green Algae. J. Biol. Chem. 2009; 284:36620–36627. [PubMed: 19846550]
17. Noth J, Krawietz D, Hemschemeier A, Happe T. Pyruvate:Ferredoxin Oxidoreductase Is Coupled to Light-independent Hydrogen Production in *Chlamydomonas reinhardtii*. J. Biol. Chem. 2013; 288:4368–4377. [PubMed: 23258532]
18. Lubitz W, Reijerse E, van Gastel M. [NiFe] and [FeFe] hydrogenases studied by advanced magnetic resonance techniques. Chem. Rev. 2007; 107:4331–4365. [PubMed: 17845059]
19. Kamp C, et al. Isolation and first EPR characterization of the [FeFe]-hydrogenases from green algae. Biochim. Biophys. Acta. 2008; 1777:410–416. [PubMed: 18355437]
20. Silakov A, Kamp C, Reijerse E, Happe T, Lubitz W. Spectroelectrochemical characterization of the active site of the [FeFe] hydrogenase HydA1 from *Chlamydomonas reinhardtii*. Biochemistry. 2009; 48:7780–7786. [PubMed: 19634879]
21. Adamska A, et al. Identification and characterization of the “super-reduced” state of the H-cluster in [FeFe] hydrogenase: a new building block for the catalytic cycle? Angew. Chem., Int. Ed. 2012; 51:11458–11462.
22. Shepard EM, et al. [FeFe]-hydrogenase maturation: HydG-catalyzed synthesis of carbon monoxide. J. Am. Chem. Soc. 2010; 132:9247–9249. [PubMed: 20565074]
23. Mulder DW, et al. Insights into [FeFe]-hydrogenase structure, mechanism, and maturation. Structure. 2011; 19:1038–1052. [PubMed: 21827941]
24. Razavet M, et al. Transient FTIR spectroelectrochemical and stopped-flow detection of a mixed valence (Fe(I)-Fe(II)) bridging carbonyl intermediate with structural elements and spectroscopic characteristics of the di-iron sub-site of all-iron hydrogenase. Chem. Commun. (Cambridge, U. K.). 2002:700–701.
25. Winkler M, Esselborn J, Happe T. Molecular basis of [FeFe]-hydrogenase function: An insight into the complex interplay between protein and catalytic cofactor. Biochim. Biophys. Acta. 2013 PMID: 23507618.

## References for Online Methods

26. Akhtar MK, Jones PR. Deletion of *iscR* stimulates recombinant clostridial Fe-Fe hydrogenase activity and $H_2$-accumulation in *Escherichia coli* BL21(DE3). Appl. Microbiol. Biotechnol. 2008; 78:853–862. [PubMed: 18320190]
27. Kuchenreuther JM, et al. High-yield expression of heterologous [FeFe] hydrogenases in *Escherichia coli*. PLoS One. 2010; 5:e15491. [PubMed: 21124800]
28. von Abendroth G, et al. Optimized over-expression of [FeFe] hydrogenases with high specific activity in *Clostridium acetobutylicum*. Int. J. Hydrogen Energy. 2008; 33:6076–6081.
29. Gulis G, Narasimhulu KV, Fox LN, Redding KE. Purification of $His_6$-tagged Photosystem I from *Chlamydomonas reinhardtii*. Photosynth. Res. 2008; 96:51–60. [PubMed: 18175204]
30. Kuhlgert S, Drepper F, Fufezan C, Sommer F, Hippler M. Residues PsaB Asp612 and PsaB Glu613 of photosystem I confer pH-dependent binding of plastocyanin and cytochrome $c_6$. Biochemistry. 2012; 51:7297–7303. [PubMed: 22920401]
31. Schmidt M, Contakes SM, Rauchfuss TB. First generation analogues of the binuclear site in the Fe-only hydrogenases: $Fe_2(\mu\text{-}SR)_2(CO)_4(CN)_2^{2-}$. J. Am. Chem. Soc. 1999; 121:9736–9737.
32. Razavet M, et al. All-iron hydrogenase: synthesis, structure and properties of {2Fe3S}-assemblies related to the di-iron sub-site of the H-cluster. Dalton Trans. 2003:586–595.
33. Hemschemeier A, Melis A, Happe T. Analytical approaches to photobiological hydrogen production in unicellular green algae. Photosynth. Res. 2009; 102:523–540. [PubMed: 19291418]
34. Zijlstra WG, Buursma A. Spectrophotometry of Hemoglobin: Absorption Spectra of Bovine Oxyhemoglobin, Deoxyhemoglobin, Carboxyhemoglobin, and Methemoglobin. Comp. Biochem. Physiol., B: Comp. Biochem. 1997; 118:743–749.

35. Reijerse E, Lendzian F, Isaacson R, Lubitz W. A tunable general purpose Q-band resonator for CW and pulse EPR/ENDOR experiments with large sample access and optical excitation. J. Magn. Reson. 2012; 214:237–243. [PubMed: 22196894]



Europe PMC Funders Author Manuscripts

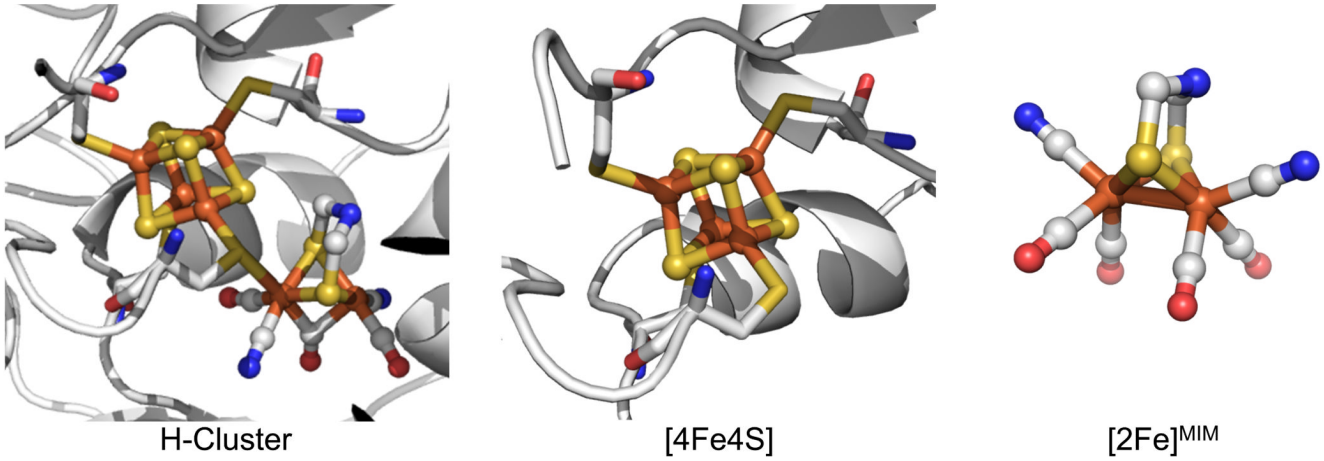


**Figure 1. The H-cluster is assembled from a regular [4Fe-4S]-cluster and a unique [2Fe]-subcluster**

The synthetic [2Fe]-subcluster ([2Fe]$^{MIM}$) differs from the binuclear subsite of the H-cluster by an additional CO-group. Models of the H- and the [4Fe-4S]-clusters were generated in PyMOL on the basis of PDB structures 3C8Y and 3LX4, respectively. [2Fe]$^{MIM}$ was also modeled in PyMOL according to information given in [11]. Some amino acids were deleted to provide an unobstructed view of the clusters. The metal clusters are in the ball-and-stick representation, the coordinating cysteines are shown as sticks. Orange: iron, yellow: sulfur, gray: carbon, blue: nitrogen, red: oxygen.

Europe PMC Funders Author Manuscripts

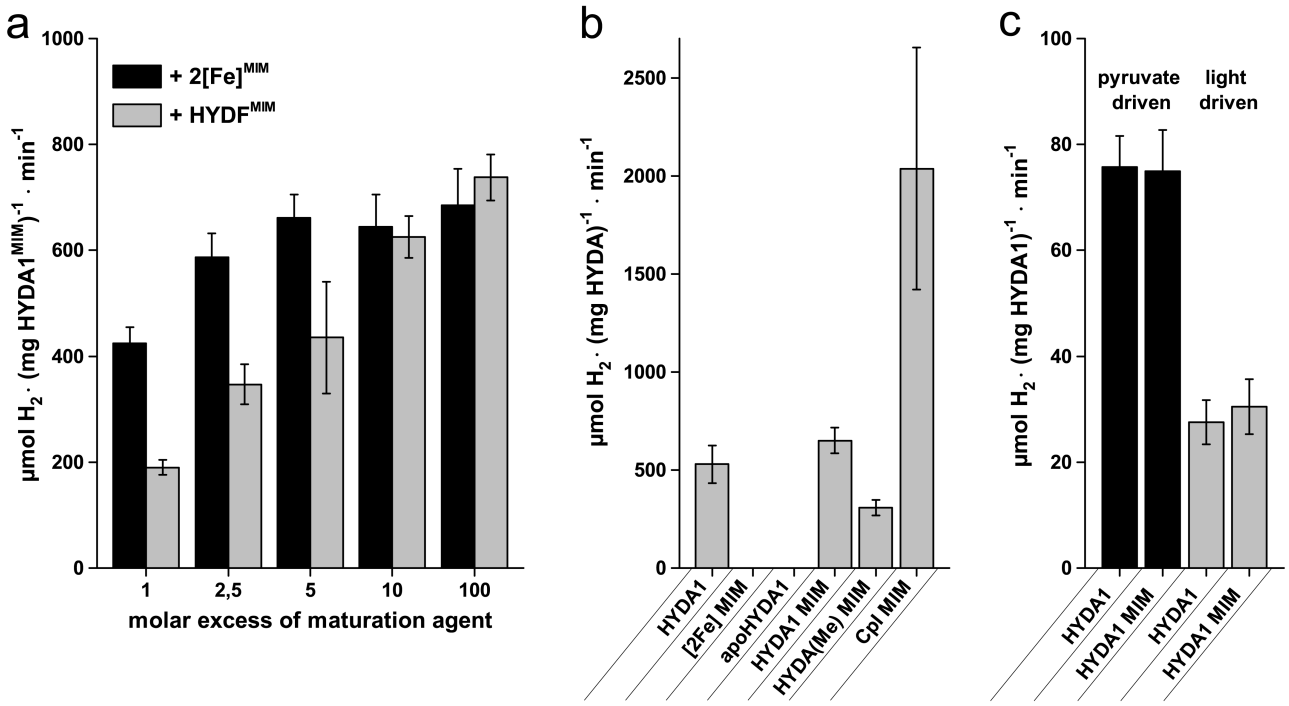


**Figure 2. Various types of HYDA enzymes can be spontaneously activated by [2Fe]$^{MIM}$ and behave like the natural enzymes**

**a**, Specific $H_2$ evolution activities of *C. reinhardtii* HYDA1 after combination of apoHYDA1 with [2Fe]$^{MIM}$ alone or [2Fe]$^{MIM}$-loaded HYDF. Molar ratios are indicated on the x-axis. **b**, HYDA1$^{MIM}$ reached the same specific activity as HYDA1 heterologously produced in *C. acetobutylicum*[10] while neither [2Fe]$^{MIM}$ nor apoHYDA1 showed any activities. [2Fe]$^{MIM}$ also activated apoHYDA enzymes of *M. elsdenii* (HYDA Me MIM) and *C. pasteurianum* (CpI MIM). We measured $H_2$ evolution using reduced methyl viologen as electron donor. **c**, $H_2$ production was also achieved in reconstitution assays including pyruvate, acetylCoA, pyruvate:ferredoxin oxidoreductase PFR1 and ferredoxin PETF in the dark[17] (pyruvate-driven) or with photosystem 1 (PS1), PETF and the necessary PS1 reducing agents[16] in the light (light-driven). **a – c,** All values shown are mean values from at least four independent experiments. Error bars indicate the standard deviation.

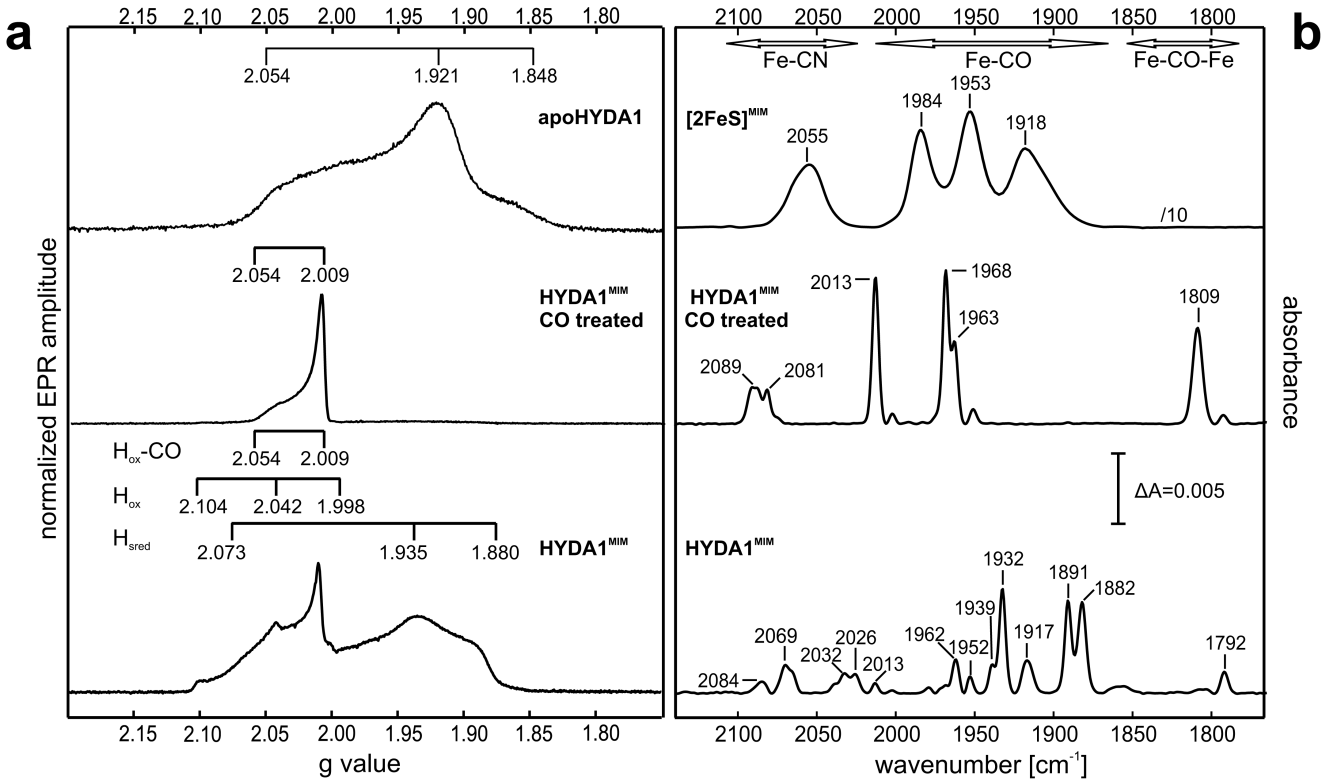


**Figure 3. The chemically reconstituted H-cluster is virtually indistinguishable from the native form**

**a**, EPR-spectra of apoHYDA1,HYDA1$^{MIM}$ in the CO-inhibited $H_{ox}$-CO state and as isolated HYDA1$^{MIM}$ comprising all EPR active states. **b**, FTIR spectra of [2Fe]$^{MIM}$ in solution,of CO-treated HYDA1$^{MIM}$ and as isolated HYDA1$^{MIM}$ . EPR simulations for each state are shown[19,21] in the supplementary results (Supplementary Fig. 2a). The g-values are indicated above the spectra. The assignments of the FTIR signals to the different redox states are collected in Supplementary Fig. 2b. All spectra were recorded on two independently prepared samples. One representative result is shown.